

University of Pretoria Department of Economics Working Paper Series

Predicting the Conditional Distributions of Inflation and Inflation Uncertainty in South Africa: The Role of Climate Risks

Mehmet Balcilar University of Florida Kenny Kutu University of Pretoria Sonali Das University of Pretoria Rangan Gupta University of Pretoria Working Paper: 2025-29 August 2025

Department of Economics University of Pretoria 0002, Pretoria South Africa

Tel: +27 12 420 2413

Predicting the Conditional Distributions of Inflation and Inflation Uncertainty in South Africa: The Role of Climate Risks

Mehmet Balcilar*, Kenny Kutu**, Sonali Das*** and Rangan Gupta****

Abstract

This paper analyzes the predictive effect of climate risks on inflation and inflation uncertainty in an inflation targeting emerging economy through a multivariate nonparametric higher-order causality-in-quantiles test. In this regard, we obtain a monthly Google Trends search-based Climate Attention Index for South Africa (CAI-SA), which incorporates both local and global terms dealing with physical and transition risks between January 2004 and September 2024. Using the CAI-SA, we find that linear Granger causality tests fail to show any evidence of prediction of overall and food and non-alcoholic beverages inflation rates, due to model misspecifications from nonlinearity and structural breaks. However, the robust multivariate nonparametric framework depicts statistically significant predictability over the entire conditional distribution of not only the two inflation rates, but also their respective volatilities, i.e., squared values. The strongest predictive impact is observed at the tails of the conditional distributions of the first- and second-moment of the two inflation rates. Our findings, in general, are robust to alternative definitions of inflation volatility, exclusion of the control variables, different methods of construction of the CAI, and a bootstrapped version of the test to account for size distortion and low power. Analyses involving signs of the causal impact reveal significant positive association between the CAI-SA and the inflation rates and their volatilities, thus having serious implications for monetary policy decisions in South Africa in the wake of heightened climate risks.

Keywords: Climate Attention Index; Inflation; Inflation Uncertainty; Higher-Order

Multivariate Causality-in-Quantiles Test; South Africa

JEL Codes: C22, C53, E31, Q54

_

^{*} Department of Economics and Business Analytics, University of New Haven, West Haven, Connecticut, United States; Department of Economics, OSTIM Technical University, Ankara, Türkiye. Email: mbalcilar@newhaven.edu.

^{**} Department of Business Management, University of Pretoria, Pretoria, 0002, South Africa. Email: u19122943@tuks.co.za.

^{***} Department of Business Management, University of Pretoria, Pretoria, 0002, South Africa. Email: sonali.das@up.ac.za.

^{****} Department of Economics, University of Pretoria, Pretoria, 0002, South Africa. Email: rangan.gupta@up.ac.za.

1. Introduction

Climate change remains one of the most complex challenges facing humanity in the 21st century. The emergence of physical climate risks in particular are a cause for concern, with hazardous weather events such as heatwaves and floods increasing in their frequency and magnitude (AghaKouchak et al., 2020; Grab and Nash, 2024). Extensive climate econometric research modelling the effects of physical climate risks on economic growth often suggest negative impacts, where developing countries are especially prone to adverse economic outcomes (Alessandri and Mumtaz, 2022; Huber et al., 2023). While the influence of both acute and chronic natural hazards on output is well-established, their effects on inflation have received limited attention. Theoretically, extreme weather events influence aggregate demand and aggregate supply dynamics, which subsequently affect inflation (Batten, 2018; Ciccarelli and Marotta, 2024). On the supply side, negative shocks emanating from natural disasters decrease agricultural production, which in turn increases food prices, dampens economic activity, and reduces labor productivity. Damaged transportation infrastructure further disrupts supply chains and increases distribution costs, altogether culminating in inflationary impacts. On the demand side, disaster events may lead to a reduction in inflation through Keynesian supply shocks. These shocks increase the risk aversion of economic agents, thus reducing their consumption and investments, even in the presence of fiscal support. Consequently, assessing the inflationary impact of climate risks remains an empirical issue. Attempts to empirically ascertain the climate-inflation nexus often report contradictory findings, especially in international panels of heterogeneous developed and emerging countries (Cashin et al., 2017; Parker, 2018; Faccia et al., 2021; Mukherjee and Ouattara, 2021; Kabundi et al., 2022; Cevik and Jalles, 2023; Liao et al., 2024; Qi et al., 2025). In this regard, one may arrive at more definitive answers through country-specific studies, such as those conducted for European nations and the United States (US) (Ciccarelli et al., 2023; Sheng et al., 2024; Kim et al., 2025).

Given this context, this paper analyzes the causal effect of climate risks on the movements of inflation in an emerging state, namely South Africa. As a major exporter of commodities such as coal, gold, iron ore, and platinum, South Africa's mining sector and broader economy has historically been powered by fossil fuels, primarily coal. The country subsequently ranks among the leading emitters of carbon dioxide globally, resulting in heightened exposure to climate transition risks (Wu et al., 2024). Additionally, the semi-arid climatic conditions in South Africa remain a major proponent for magnified exposure to physical risk. For instance, a projected 1.5°C increase in global average temperature equates to a 3 °C increase in South Africa's average temperature. Such climate anomalies may result in more frequent extreme weather events in the country¹, as witnessed in recent years. At the same time, South Africa is an inflation targeting economy since February 2000 (with an original target band of 3%-6%), hence, the effect of climate risks on inflation has paramount importance from the perspective of monetary policy decisions, as recently acknowledged by the South African Reserve Bank (SARB) in its Annual Report of 2023/2024.² Furthermore, the SARB, while discussing the importance of climate change in South Africa, has stressed not only on physical, but also transition risks associated with a move towards a "greener economy" (SARB, 2025) through greater reliance on renewables for energy generation, and carbon tax.

_

See: https://www.bcg.com/publications/2022/how-south-african-mining-can-address-climate-change-challenges.

² See the discussions in: https://resbank.onlinereport.co.za/2024/downloads/Addressing-climate-change-risks.pdf, and https://www.resbank.co.za/en/home/about-us/climate-change.

Though less researched than the effects of physical risks on inflation, transition risks can also have inflationary or deflationary impacts. Global transition efforts towards lower carbon emitting production processes require metal and mineral-intensive green technologies. A subsequent supply squeeze occurs, where rising demand for metals such as copper, lithium and cobalt for green technologies is met by supply bottlenecks, resulting in what is often referred to as "greenflation" (Schnabel, 2022). Conversely, in their textbook New Keynesian model Ferrari and Nispi Landi (2024) found that increases in carbon taxes today raise inflation, but expected future carbon tax increases decrease current demand, resulting in downward pressure on prices. Through numerical simulations, they further find stronger demand-suppressing effects, thus causing green transitions to be deflationary under conditions of climate policy certainty. However, where there is uncertainty surrounding climate policies, inflationary impacts are expected (Huang and Tereza Punzi, 2024). Within the South African climate transition risk context, an inflationary outcome is also highly likely owing to a high degree of uncertainty surrounding climate-related policymaking in the country (Ji et al., 2024; Kutu et al., forthcoming).³

In line with the existing literature on devising metrics for physical and transition climate risks via textual analysis (see, for example, Engle et al. (2020), Faccini et al. (2023), Bua et al. (2024)), we create a climate attention index for South Africa (CAI-SA) based on Google Trends (GT) searches of large number of terms relating to physical and transition risks, thus making it an appropriate measure to capture overall climate risks (Ben Ameur et al., 2024). In this regard, our search involved both country-specific and global terms, given that South Africa is a small open economy impacted by international shocks in a highly interconnected supply-chain system (Burriel et al., 2024), and is also motivated by Bilal and Känzig (forthcoming), who stresses that global rather than local climate factors drive extreme climatic events.

In theory, with climate risks serving as proxies for rare disasters, the possible positive effect on inflation volatility could originate from a model of inattention put forth by Sundaresan (2024). Here, agents gather information to decide how to prepare for possible scenarios, while ignoring unlikely events. Hence, the occurrence of rare disasters does not resolve, but instead increases general uncertainty (Sheng et al., 2022; Ma et al., 2024; Zhang et al., 2024). Inflation uncertainty in South Africa has played an important role in inflationary outcomes, especially in the post inflation-targeting era (Ben Nasr et al., 2015; van der Westhuizen, 2023). The effects of climate risks on inflation volatility is an equally important consideration in monetary policy decisions as it can enhance inflation persistence following physical and transition risks shocks. If these shocks are inflationary, they may result in prolonged intervention by the SARB. In this context, our methodology also allows us to investigate the predictive impact of climate risks on the second-moment of inflation, i.e., inflation uncertainty, due to climate risks.

This paper presents a novel approach to analyzing the effects of climate risks on the conditional distribution of inflation and inflation volatility in South Africa, primarily through a higher-order nonparametric causality-in-quantiles model. The significant contribution of the food and non-alcoholic beverages sector (19.88%) to the country-wide Consumer Price Index (CPI) computation⁴, in tandem with the well-established physical risks exposure of South Africa's

³ In fact, using a newspapers based index of Climate Policy Uncertainty (CPU), created by Ji et al. (2024) for South Africa (besides 11 other G20 economies), available at: http://www.cnefn.com/data/download/climate-risk-database/, we found a significant (at the 1% level) positive association (given a coefficient of 0.7776) with the year-on-year overall inflation rate (details of which is provided in Section 2) using an Ordinary Least Squares (OLS) regression over the monthly period of July 2018 to December 2023.

⁴ The reader is referred to: https://www.statssa.gov.za/publications/P01415/P014152023.pdf.

agriculture sector motivate the approach to investigate the impacts of climate risks on aggregate and food and non-alcoholic beverages sector associated inflation. Additionally, as climate risks have an immediate effect on agriculture productivity, the focus on the food and non-alcoholic beverages sector enables the evaluation of its likely contribution on the overall inflation in the wake of extreme climate events. Moreover, with expenditure on food and beverages accounting for nearly 30% of the total expenditure of poorer households (2022/2023 Income and Expenditure Survey⁵), understanding inflation variability in this sector is a major concern from the distributional dimension of climate shocks perspective.

The preview of our results show that indeed there is robust evidence that physical and transition climate risks, which are captured by the attention index, not only predict the level of both the overall and the food and beverages inflation rates, but also their associated volatilities throughout their respective conditional distributions. The remainder of the paper is organized as follows: Section 2 outlines the data used in our analysis; Section 3 is devoted to the elucidation of the methodology used; Section 4 presents the empirical findings; and finally in Section 5 we present our concluding comments of the work presented in this paper.

2. Data

In this study, the two dependent variables of interest are the overall inflation rate (INFL), and the food and non-alcoholic beverages inflation rate (INFLF). Both INFL and INFLF are in percentages, and we utilize the year-on-year changes of the natural logarithm of the corresponding seasonally-adjusted CPIs, multiplied by 100. The two macroeconomic control variables used are in line with a standard small-scale monetary model, for which we use the year-on-year changes in the natural logarithmic values of the seasonally-adjusted manufacturing production index (MPG) to reflect monthly economic growth, and the level of the seasonally-unadjusted 3-month Treasury bill rate in percentage (STR) that reflects the status of short-term interest rate, and hence, are a reflection of monetary policy decisions. The required underlying raw data are obtained from the online data segment of the SARB⁶, and the four variables of interest, namely INFL, INFLF, MPG and STR are presented in Figure 1.

[INSERT FIGURE 1]

The main predictor variable in our econometric analyses is a GT-based attention index, namely the CAI-SA, constructed to measure physical and transition climate risks in South Africa. Recognizing the ability for GT — a freely accessible, open source, providing real-time data on public attention or interest on a plethora of topics, we construct our CAI-SA using the relative search volume index (SVI) from GT. Our GT-based CAI-SA considers both local and global climate related search terms. As such, we select thirty globally relevant climate-related terms present in the Climate Change Vocabulary (CCV) compiled by Lin and Zhao (2023). And, to identify locally relevant climate-related terms, the South African government web repository was accessed to identify key documents (namely, the Climate Change Act 22 of 2024, and the Climate Change Bill B9-2022) and localized glossaries, to build a comprehensive CCV list for the CAI-SA. Subsequently, 21 additional terms which were not explicitly listed by Lin and Zhao (2023) were identified and included in the CCV list for development of the CAI-SA.

⁵ See: https://www.statssa.gov.za/publications/P0100/P01002022.pdf.

⁶ Accessible via: https://www.resbank.co.za/en/home/what-we-do/statistics/releases/economic-and-financial-data-for-south-africa.

⁷ See: https://www.gov.za/documents.

Finally, considering South Africa's reliance on coal and other fossil fuels, and the subsequent efforts to ensure a renewable energy transition, the terms "just transition" and "just energy transition" were included in the final CCV list. In Table 1, we categorize all 53 CCV terms included in the construction of the CAI-SA in accordance with their relation to either physical or transition risks.

[INSERT TABLE 1]

After the compilation of the final CCV list, we collected GT data for the 53 search terms, which were confined to searches emanating from South Africa, from January 2004 to September 2024. Using average GT SVI values associated with each search term, we plotted a word cloud in Figure 2, where terms with higher mean values (which can be associated with higher relative search volumes) are plotted larger than words with lower mean values.⁸

[INSERT FIGURE 2]

To ensure comparability between the search terms used in the construction of the CAI-SA, we standardize the raw SVI series for each CCV term by demeaning and scaling each series by its standard deviation, before applying Principal Component Analysis (PCA) to obtain our CAI-SA, which is plotted in Figure 3.

[INSERT FIGURE 3]

As is customary in the development of indexes, we visually analyse the ability for the CAI-SA to capture climate-related events through observed peaks. To ensure rigour in our analysis, we preselect 11 local and international climate-related events (listed in Table 3), with the expectation that peaks in the CAI-SA will occur around the date of key climate-related news events, implying the ability of the index to track attention on real-world events. The categorization of climate-related policy events by Chen et al. (2024) lay the foundation for the selection of international climate-related news events. The selection of key local events primarily considers risks, reflected through some major climate policy shifts in South Africa occurring within the sample period. Figure 3 depicts the CAI-SA, annotated in relation to key climate-related events occurring locally and internationally. We find that the index was able to capture all the preselected major climate-related events through its peaks. Further, there is consistent emergence of pronounced negative peaks, which occur in the third quarter of each year in the series, generally coinciding with Conference of Parties (COP) meetings, dealing with issues of international climate change policy negotiations. Conversely, during the period of COP17, which was hosted in Durban, South Africa, the CAI-SA index displayed a positive peak. More interestingly, upon enforcement of the Paris Agreement in November 2016, the CAI-SA displayed a positive peak.

[INSERT TABLE 2]

As can be seen from Figure 3, some of the search terms could have added seasonality to the CPI-SA index, hence, we use the Seasonal and Trend decomposition using LOESS (STL)

⁸ Where mean SVI for a search term for our sample period is less than 1, the term was excluded from the word cloud.

approach of Cleveland et al. (1990) to filter out the seasonal pattern in this series, and utilize this deseasonalized version in our econometric analyses to ensure robust empirical findings.⁹

Table 3 summarizes the variables of interest, i.e., the dependent variables: INFL and INFLF, and the predictor: CAI-SA, as well as the two control variables of MPG and STR. As can be seen from the table, all the variables are non-normal based on the rejection of the null hypothesis of normality as per the Jarque-Bera test, and provides an initial motivation to look at a quantiles-based approach given, in particular, the heavy tails of the dependent variables: INFL and INFLF. Furthermore, the Augmented Dickey-Fuller (ADF; Dickey and Fuller, 1979) unit root test ensures that all the variables under consideration are stationary and, hence, are fit to be utilized in the nonparametric causality-in-quantiles test.

[INSERT TABLE 3]

3. Methodology

In this section, we present the multivariate k-th order nonparametric causality-in-quantile test of Balcilar et al. (2022), which augments the original bivariate test developed by Balcilar et al. (2018).

We denote the dependent variable (INFL or INFLF) as u_t , the predictor variable (CAI-SA) as v_t , and n possible predictors as $W_t \equiv \left(w_{1,t}, w_{2,t} \dots, w_{n,t}\right)'$, (which are the control variables MPG and STR in our case). Therefore, the multivariate quantile causality is defined using: $U_{t-1} \equiv (u_{t-1}, \dots, u_{t-p})'$, and $W_{t-1} \equiv (w_{t-1}, \dots, w_{t-p})'$ and $W_{t-1} \equiv (w_{t-1}, \dots, w_{t-p}, \dots, w_{n,t-p}, \dots, w_{n,t-p})'$. Following the notation $Z_t = (U_t', V_t', W_t')'$, $X_t = (U_t', W_t')'$, the conditional distribution of u_t given Z_{t-1} and u_t given $Z_{t-1} \setminus V_{t-1} \equiv X_{t-1} \equiv (U_{t-1}', W_{t-1}')'$ can be denoted by $F_{u_t|Z_{t-1}}(u_t|Z_{t-1})$ and $F_{u_t|Z_{t-1}\setminus V_{t-1}}(u_t|Z_{t-1}\setminus V_{t-1})$, respectively, where $Z_{t-1} \setminus V_{t-1}$ implies the information set which does not include V_{t-1} . Let also the θ -th conditional quantile of u_t , given the information set \cdot , be denoted by $Q_{\theta}(\cdot)$. Following Nishiyama et al. (2011) and Jeong et al. (2012), Granger non-causality-in-quantile is defined as: v_t does not cause u_t in the θ -th quantile, if:

$$Q_{\theta}(u_{t}|Z_{t-1}) = Q_{\theta}(u_{t}|Z_{t-1}\backslash V_{t-1}) \tag{1}$$

while Granger causality-in-quantile is defined as: v_t is a prima facie cause of u_t in the θ -th quantile, if:

$$Q_{\theta}(u_{t}|Z_{t-1}) \neq Q_{\theta}(u_{t}|Z_{t-1}\backslash V_{t-1}),\tag{2}$$

Eq. (1) and Eq. (2) can be equivalently expressed as:

$$H_0: P\{F_{u_t|Z_{t-1}}\{Q_{\theta}(Z_{t-1}\backslash V_{t-1})|Z_{t-1}\} = \theta\} = 1$$
(3)

$$H_1: P\{F_{u|Z_{t-1}}\{Q_{\theta}(Z_{t-1}\setminus V_{t-1})|Z_{t-1}\} = \theta\} < 1$$

$$\tag{4}$$

⁹ The raw CAI-SA and the seasonally-adjusted CAI-SA has a statistically significant (at the 1% level, given a p-value of 0.0000) correlation coefficient of 0.8224.

where the θ -th quantiles are denoted as $Q_{\theta}(Z_{t-1}) \equiv Q_{\theta}(u_t|Z_{t-1})$ and $Q_{\theta}(Z_{t-1}\setminus V_{t-1}) \equiv Q_{\theta}(u_t|Z_{t-1})$ $Q_{\theta}(X_{t-1}) \equiv Q_{\theta}(u_t|Z_{t-1}\setminus V_{t-1})$, which satisfy $F_{u_t|Z_{t-1}}\{Q_{\theta}(Z_{t-1})|Z_{t-1}\} = \theta$ with probability

In order to construct the test, we consider metric: $J = \{\epsilon_t E(\epsilon_t | Z_{t-1}) f_Z(Z_{t-1})\}$, where $f_Z(Z_{t-1})$ is the marginal density. The regression error ϵ_t emerges based on the null in Eq. (3), which can be true if and only if $E[\mathbf{1}\{u_t \leq Q_{\theta}(Z_{t-1} \setminus V_{t-1}) | Z_{t-1}\}] = \theta$, or equivalently $\mathbf{1}\{u_t \leq Q_{\theta}(Z_{t-1} \setminus V_{t-1})\} = \theta + \epsilon_t$, where $\mathbf{1}\{\cdot\}$ is the indicator function. Thus, the metric J can be specified as:

$$J = E[\{F_{u_t|Z_{t-1}}\{Q_{\theta}(Z_{t-1}\backslash V_{t-1})|Z_{t-1}\} - \theta\}^2 f_Z(Z_{t-1})]$$
(5)

The empirical counterpart of Eq. (5), based on Jeong et al. (2012), is constructed as follows:

$$\hat{J}_T = \frac{1}{T(T-1)h^m} \sum_{t=p+1}^T \sum_{s=p+1, s \neq t}^T K\left(\frac{Z_{t-1} - Z_{s-1}}{h}\right) \hat{\epsilon}_t \hat{\epsilon}_s \tag{6}$$

where $K(\cdot)$ is the kernel function with bandwidth h; T is the sample size; m is the dimension of Z_t , and $\hat{\epsilon}_t$ is the unknown regression estimate, which is constructed as:

$$\hat{\epsilon}_t = \mathbf{1}\{u_t \le \hat{Q}_{\theta}(Z_{t-1} \setminus V_{t-1})\} - \theta \tag{7}$$

where $\hat{Q}_{\theta}(Z_{t-1} \setminus V_{t-1})$ is an estimate of the θ -th conditional quantile. Following arguments similar Jeong et al. (2012), $Th^{m/2} \hat{j}_T \stackrel{d}{\to} N(0, \sigma_0^2)$. In general, causality in conditional mean (first-moment) implies causality in higher order moments, but not vice versa. Thus, a sequential testing approach for causality in k-th moment is adopted as follows:

$$H_{0}: P\left\{F_{u_{t}^{k}|Z_{t-1}}\{Q_{\theta}(Z_{t-1}\backslash V_{t-1})|Z_{t-1}\} = \theta\right\} = 1 \qquad k = 1, 2, ..., K$$

$$H_{1}: P\left\{F_{u_{t}^{k}|Z_{t-1}}\{Q_{\theta}(Z_{t-1}\backslash V_{t-1})|Z_{t-1}\} = \theta\right\} < 1 \qquad k = 1, 2, ..., K$$

$$(9)$$

$$H_1: P\left\{F_{u_t^k|Z_{t-1}}\{Q_{\theta}(Z_{t-1}\backslash V_{t-1})|Z_{t-1}\} = \theta\right\} < 1 \qquad k = 1, 2, \dots, K$$

$$(9)$$

The test statistic is formulated as in Eq. (6) by replacing u_t with u_t^k . It is important to note that $J \ge 0$, i.e. the equality holds if and only if H_0 in Eq. (3) or Eq. (8) is true; while J > 0 holds under the alternative H_1 in Eq. (4) or Eq. (9). We, therefore, consider a re-scaled version using:

$$\hat{\sigma}_0 = \sqrt{2}\theta (1 - \theta) \sqrt{\frac{1}{T(T - 1)h^m}} \sqrt{\sum_{t=p+1, t \neq s}^{T} K^2 \left(\frac{Z_{t-1} - Z_{s-1}}{h}\right)}$$

and establish that: $\hat{t}_T = \frac{\hat{j}_T}{T^{-1}h^{-m/2}\sigma_0} \stackrel{d}{\to} N(0,1)$.

The θ -th quantile of u_t , is estimated as $\hat{Q}_{\theta}(Z_{t-1} \setminus V_{t-1}) = \inf\{u_t : \hat{F}_{u_t \mid Z_{t-1} \setminus V_{t-1}}(u_t \mid Z_{t-1} \setminus V_{t-1})\}$ $V_{t-1} \ge \theta$, where the Nadaraya–Watson kernel estimator $\hat{F}_{u_t|Z_{t-1}\setminus V_{t-1}}(\cdot)$ is given by:

$$\hat{F}_{u_{t}|Z_{t-1}\setminus V_{t-1}}(u_{t}|Z_{t-1}\setminus V_{t-1}) = \frac{\sum_{s=p+1,t\neq s}^{T} L\left(\frac{X_{t-1}-X_{s-1}}{b}\right) \mathbf{1}\{u_{s} \leq u_{t}\}}{\sum_{s=p+1,t\neq s}^{T} L\left(\frac{X_{t-1}-X_{s-1}}{b}\right)}$$

with $L(\cdot)$ denoting the kernel function and b the bandwidth.

In implementing this test, on the basis of our model specifications, we have: $(u_t)^{(l)} = m(Z_{t-1}) + \epsilon_t$, where u_t represents the INF or INFLF. Causality-in-mean is defined as m = 1, while causality-in-variance involves l = 2.

The empirical implementation of the tests above involve the specification of three main parameters: the bandwidths (h and b), the lag order (p), and the kernel types for $K(\cdot)$ and $L(\cdot)$. The lag order (p) is selected based on the Schwarz Information Criterion (SIC), with h and b determined by the leave-one-out least-squares cross-validation, and we use Gaussian kernels for $K(\cdot)$ and $L(\cdot)$.

Tests for Granger causality-in-quantiles are based on an asymptotic normal approximation to the test statistic \hat{J}_T under the null. However, several studies have found this approximation to be untrustworthy in finite samples. Indeed, Li and Wang (1998) report that the convergence of such nonparametric test statistics to their limiting normal distribution can be very slow (to the order of $T^{-1/10}$ even in a bivariate case with one lag and bandwidth of $h = T^{-1/5}$). Consequently, the use of nominal normal critical values frequently results in severe size distortions in realistic sample sizes. Hsiao et al. (2007) also report that the asymptotic N(0,1) approximation has a tendency to underestimate the actual rejection probability of the test for moderate T, even when T is quite large. These results motivate the application of bootstrap methods as a way of obtaining a better approximation to the finite-sample null distribution of the test statistic. By resampling from the data to obtain an empirical distribution for \hat{J}_T under H_0 , the bootstrap can rectify the distortion and yield more accurate critical values. The technical details of a residual-based bootstrap procedure for the quantile causality test, which will replace the asymptotic normal approximation with a simulated distribution, is presented in Appendix B of this paper.

4. Empirical Findings

To ensure the completeness and comparability of results from our initial utilising of the multivariate k-th order nonparametric causality-in-quantiles framework, we conducted the linear Granger causality test running from climate risks to overall and food and non-alcoholic beverages inflation rates. We found that, the null of no-Granger causality from CAI-SA to INFL and INFLF, with MPG and STR as control variables, cannot be rejected even at the 10% level of significance, given the corresponding values of the $\chi^2(1)$ test statistics (p-value), given p=1 as per the SIC, to be equal to 0.0586 (0.8087), and 0.6689 (0.4134).

The standard Granger causality test, shows a lack of predictability from our measure of climate risks onto the two inflation rates under consideration. The finding of non-causality may allude to model misspecifications stemming from the assumption of linearity in the predictive relationships. This necessitated a test for the presence of nonlinearity in the relationship between INFL and INFLF with CAI-SA, controlling for MPG and STR in the model. A BDS test on the residuals from the two initial linear models assessed whether the null hypothesis of *i.i.d.* residuals at various dimensions (*m*) could be rejected or not (Brock et al., 1996). Results of the BDS test presented in Table 4, provide strong evidence of nonlinearity for both INFL and INFLF, such that we reject the null hypothesis of linearity (*i.i.d.* residuals) at the 1% level of significance. The BDS test ultimately confirms that the linear model utilized for tests of Granger causality is indeed a misspecification, owing to uncaptured nonlinearity. Consequently, further causal inference must implore a nonlinear model, whereby the nonparametric causality-in-quantiles approach is followed. Intuitively, the nonlinearity

between inflation and climate risks should not be surprising in light of prices being known to be downward rigid, and increases and decreases in climate shocks have been shown asymmetric inflationary effects (Sheng et al., 2024; Kim et al., 2025).

[INSERT TABLE 4]

Next, issues of instability in the linear models were addressed, where additional layers of misspecification could have materialized. Through the *UDmax* and *WDmax* tests, we examined the relationship between INFL and INFLF with CAI-SA, given MPG and STR in the equations of the linear Granger causality test for the presence of possible structural breaks (Bai and Perron, 2003). We found that there are one (January 2010) and four (August 2008, January 2012, February 2017, and August 2021) breaks respectively, in the relationships between INFL and CAI-SA, and between INFLF and CAI-SA. The dates of regime-change in 2017 and 2021 for INFLF can be associated with a redefinition of the South African inflation target to 4.5% from the target band of 3%-6%, and the delayed outcome of the COVID-19 pandemic, respectively. In the case of INFL, the break in 2010, and that for INFLF in 2008 is likely to have originated from the worldwide rise in commodity prices in the wake of the Global Financial Crisis in 2007-2009. The 2012 structural break in INFLF can be associated with severe weather conditions, and increases in production costs thereof, by which year the commodity price boom had tapered down. We infer that our linear Granger causality results are unreliable as instability exists within the parameter estimates over the full sample period

We relied on an inherently time varying econometric model to ensure robust inference of the causal analyses. This informed our statistical argument to utilize the nonparametric k-th order causality-in-quantiles testing method, which accommodates such misspecifications, while simultaneously providing results for the second-moment, i.e., inflation volatility (uncertainty). We present the standard normal test statistics, derived from this method, over the quantile range of 0.10 to 0.90 in Table 5 in which CAI-SA predicts the entire conditional distributions in a statistically significant manner not only for INFL and INFLF, but also for their corresponding squared-values capturing overall and, food and non-alcoholic beverages inflation volatility (or uncertainty). In the process, we highlight the superiority of a nonparametric approach, when misspecifications are present in a linear predictive framework in the form of nonlinearity and structural breaks. Interestingly, even though the entire conditional distribution of the first- and second-moment of both the INFL and INFLF rates are causally impacted by the CAI-SA, the effect (in terms of the magnitude of the test statistic) is strongest at the lower ($\theta = 0.10$)- and upper-tail($\theta = 0.90$) of the conditional distribution, and weakest at the conditional median ($\theta =$ 0.50), corresponding to the normal state of inflation. Put alternatively, climate risks carry strong predictive content for the extreme behavior of the inflation rates, which should not come as a surprise given that CAI-SA serves as a proxy for infrequent (rare) disasters or climate policyrelated events. Such events are likely to mimic tail risks, as recently noted for the US by Chavleishvili and Moench (2025), using a Quantile Vector Autoregression (QVAR) model of natural disasters. On a technical front, this u-shaped nature of the standard normal test statistics depicts the importance of using a quantiles-reliant approach relative to a conditional meanbased model, allowing us to capture the unique asymmetry in the strength of predictability due to physical and transition climate risks on the movements of the inflation rates.

[INSERT TABLE 5]

As part of an additional analysis in (Table A1) in the Appendix, we report the corresponding results from the bivariate versions of the k-th order nonparametric causality-in-quantiles test,

which involves INFL and CAI-SA. Understandably, the two-variable test statistics can be obtained in a similar fashion as described in Section 3, but now with W_t being a null-vector, i.e., without the controls MPG and STR. As observed from this table, the results are qualitatively similar to those obtained under the multivariate set-up, thus confirming the robustness of our findings when we ignore the two additional control variables defining the states of aggregate demand and supply. 10 Given the overwhelming focus on economic growth in the studies dealing with the climate-economy nexus, in Table A2 in the Appendix, we also present the causal impact of CAI-SA on MPG and its volatility, i.e., the squared value: a measure of macroeconomic uncertainty, using the multivariate higher-order nonparametric causality-in-quantiles test. We find that climate risks indeed predict the entire conditional distribution of output growth and its associated uncertainty in a statistically significant manner, while depicting a u-shaped pattern to the test statistics, just as in the case of the inflation rates. While our CAI-SA index is based on PCA applied to combine the information of the search terms, we also created two additional CAI indexes. In the first case, we took a simple average of the standardized values of the GT-based search terms for each month, while in the second, we considered a weighted average instead, with the weights being the ratio of the search value for a particular term relative to the total number of searches associated with all the terms for a particular month. We call these two indexes: CAI-SA-Average (CAI-SA-Avg.) and CAI-SA-Weighted-Average (CAI-SA-Wtd.-Avg.), respectively. Table A3 in the Appendix reports our findings from the multivariate k-th order nonparametric causality in quantiles test for INFL, based on these two alternative CAIs, and as can be seen, our results are qualitatively similar to those presented in Table 3 using the CAI-SA measure, confirming robustness of our findings to alternative ways of construction of the CAI metrics. This finding is not surprising, given the correlations between CPI-SA-Avg. and CPI-SA-Wtd.-Avg. with CAI-SA are positive and statistically significant.¹¹ Finally, given that there exists a twitter-based CAI for South Africa over a shorter period of October 2014 to December 2022, as developed by Arteaga-Garavito et al. (2023), 12 we compared the predictive ability of this index (CAI-SA-Alternate (Alt.)) with that of ours in predicting INFL and its volatility. Note that, due to a relatively small sample size of 99 observations, for this exercise, we rely on the bivariate version of the k-th-order nonparametric causality-in-quantiles test. As can be seen from Table A4, while CA-SA-Alt. is unable to depict any evidence of predictability, our measure of climate risks, i.e., CAI-SA, shows statistically significant causal impact over the quantile range of 0.30 to 0.80 of the conditional distributions of the first- and second-moment of INFL. These findings confirm the superiority of our index in terms of predicting movements in inflation for South Africa, though, an advantage of the CAI-SA-Alt. is its availability at higher (daily and weekly) frequencies and for 24 other countries, which makes it suitable for analysis of international financial market data (Steenkamp et al., forthcoming). It must be emphasized that while these additional analyses have been reported only for INFL, they produced qualitatively similar findings with INFLF, which in turn are available upon request from the authors.

¹⁰

 $^{^{10}}$ As part of the additional analyses, we recovered the conditional estimate of volatility of inflation by applying the Generalized Autoregressive Conditional Heteroskedasticity (GARCH(1,1)) on INFL. Then, in the bivariate set-up of the nonparametric causality-in-quantiles test involving the GARCH-based volatility of INFL as the dependent variable and CAI-SA as the independent variable, the test statistics, under k = 1, for $\theta = 0.10$, 0.20, 0.30, 0.40, 0.50, 0.60, 0.70, 0.80, and 0.90 was found to be, 2.7821, 3.8302, 3.9709, 4.2532, 4.3575, 3.9458, 3.7350, 3.5259, and 2.4623, respectively. In other words, our metric of climate risks continue to predict the entire conditional distribution (at the 1% level of significance, barring the upper-most quantile) of an alternative conditional measure of inflation uncertainty, instead of squared rates of inflation.

¹¹ The respective correlation coefficients (p-value) are: 0.9508 (0.0000) and 0.1254 (0.0482).

¹² The data is available at: https://sites.google.com/view/internationalclimatenews/download?authuser=0.

Reverting to our examination of the predictability of the first- and second-moment of INFL and INFLF due to CAI-SA through a multivariate k-th order nonparametric causality-inquantiles set-up. As highlighted in the earlier Granger causality-in-quantile test, the use of asymptotic normal approximations indicate that this set-up can be unreliable in finite samples. Li and Wang (1998) and Hsiao et al. (2007) determine that slow convergence and nominal critical values produce size distortions, underestimating rejection probabilities even in larger samples. Therefore, we compare the results from a bootstrapped version of the implemented test with the corresponding non-bootstrapped test, to check for the robustness of our findings. The 5% quantile-specific bootstrapped critical values have been presented in Table 6, revealing a continuation of a u-shaped pattern observed in the non-bootstrapped version. Given these bootstrapped critical values, when we compare the standard normal test statistics reported in Table 5 with the entries in Table 6, we observe that CAI-SA continues to predict the entire conditional distribution of INFL, but causal influence for INFLF is no longer observed at $\theta =$ 0.40 and 0.50. When we look at INFL² and INFLF², predictability due to CAI-SA is again lost at $\theta = 0.40$ and 0.50 for the former and at $\theta = 0.50$ for the latter at the 5% level of significance. Among the above cases of non-causality, only for $\theta = 0.40$ of INFL², we were able to obtain evidence of prediction at the 10% level, given the corresponding bootstrapped critical value of 2.3840.13 In general, our findings derived from the non-bootstrapped version of the tests of predictability, continue to be robust particularly at the tails, with some exceptions around the conditional median.

[INSERT TABLE 6]

Although a robust predictive inference is obtained from the non-bootstrapped multivariate k-th order nonparametric causality-in-quantiles test, it is also important to estimate the direction of the effect of CAI-SA on the first- and second-moment of INFL and INFLF. In doing so, we not only can ascertain the specific channels through which physical and transition risks impact inflation and its volatility, but also the associated increase or decrease in the variables of interest. Within the nonparametric framework, first-order partial derivatives are usually employed to evaluate the directions of effects. However, this results in complications due to slow convergence rates, the dimensionality, and smoothness of the underlying conditional expectation function. To address this, we utilize a summary statistic of the overall effect or global curvature sign and magnitude, as opposed to the entire derivative curve. The average derivative (AD) provides a measure of the global curvature, using the conditional pivotal quantile through either approximation or the Belloni et al. (2019) coupling approach, which enables the estimation of the partial ADs. In Figure 3, we plot the partial ADs depicting the sign of the causal effect from CAI-SA on INFL and INFLF, and their respective volatilities, along with 95% confidence bands. The effect of climate risks on the two inflation rates and their uncertainties are consistently positive over the corresponding conditional distributions. More importantly, the positive effects are all statistically significant, with the exception of the median volatility of INFL. This suggests the dominance of the aggregate supply route and "greenflation" (possibly coupled with climate policy uncertainties) associated with physical and transition risks respectively. Ultimately, the positive association of risk spillovers between disaster events and inflation, validates the underlying theory of inattention in this context.

[INSERT FIGURE 4]

¹³ The quantile-specific 10% bootstrapped critical values are available upon request from the authors.

5. Conclusion

This paper attempted to analyze the predictive impact of climate risks on inflation and inflation uncertainty (volatility) in South Africa, through a multivariate nonparametric k-th-order causality-in-quantiles test. In this regard, we first obtained a Google Trends search-based Climate Attention Index for South Africa (CAI-SA), involving both local and global terms relating with physical and transition risks, from January 2004 to September 2024, at monthly frequency. Next, using the CAI-SA, we find that while the linear Granger causality tests failed to show evidence of predicting overall or food and non-alcoholic beverages inflation rates, due to model misspecifications from nonlinearity and structural breaks. The multivariate nonparametric framework displayed statistically significant predictability over the entire conditional distribution of both inflation rates, as well as for their respective volatilities (i.e., squared values). The strongest predictive impact was observed at the tails of the conditional distributions of the first and second-moment of the two inflation rates, confirming the nature of the risks from extreme climate-related events. Our findings, in general, are robust to an alternative definition of conditional inflation volatility, the exclusion of the control variables, additional methods of construction of the CAI, and a bootstrapped version of the test to account for size distortion and low power issues of the asymptotic approximation. Furthermore, analyses involving signs of the causal impact reveal significant positive association between the CAI-SA and the inflation rates and their volatilities, confirming climate risks are inflationary in South Africa, and also have spillover impacts on to its uncertainties.

From a policy perspective, our results imply that the SARB, with its primary mandate of price stability, must be ready to undertake contractionary monetary policies in the wake of heightened climate risks to ensure that inflation remains within its target range. At the same time, with inflation uncertainty also increasing, which is known, based on existing studies, to fuel inflation further in South Africa, the climate-impact of inflation is likely to be persistent, which would also prolong the size and time-length of the monetary policy interventions. With climate risks shown to increase the level and fluctuation of inflation associated with food and non-alcoholic beverages, the importance of "correct" monetary policy decisions becomes of paramount importance to ensure minimal impact on the vulnerable poorer segment of the population. But one must realize, the associated likelihood of reduced economic activity (and heightened uncertainty): both directly from climate risks¹⁴ and tightening of interest rates, might require fiscal stimulus from the Treasury to revive output growth in the medium- to long-run.

Although the results of our analysis proved robust, it remains uncertain whether they provide out-of-sample forecasting gains. As such, extending our analysis into a forecasting exercise through Bonaccolto et al. (2018) predictive modelling framework provides potential avenues for future research.

-

¹⁴ The sign analyses revealed a negative effect on MPG and increased volatility from the CAI-SA. Complete details of these results are available upon request from the authors.

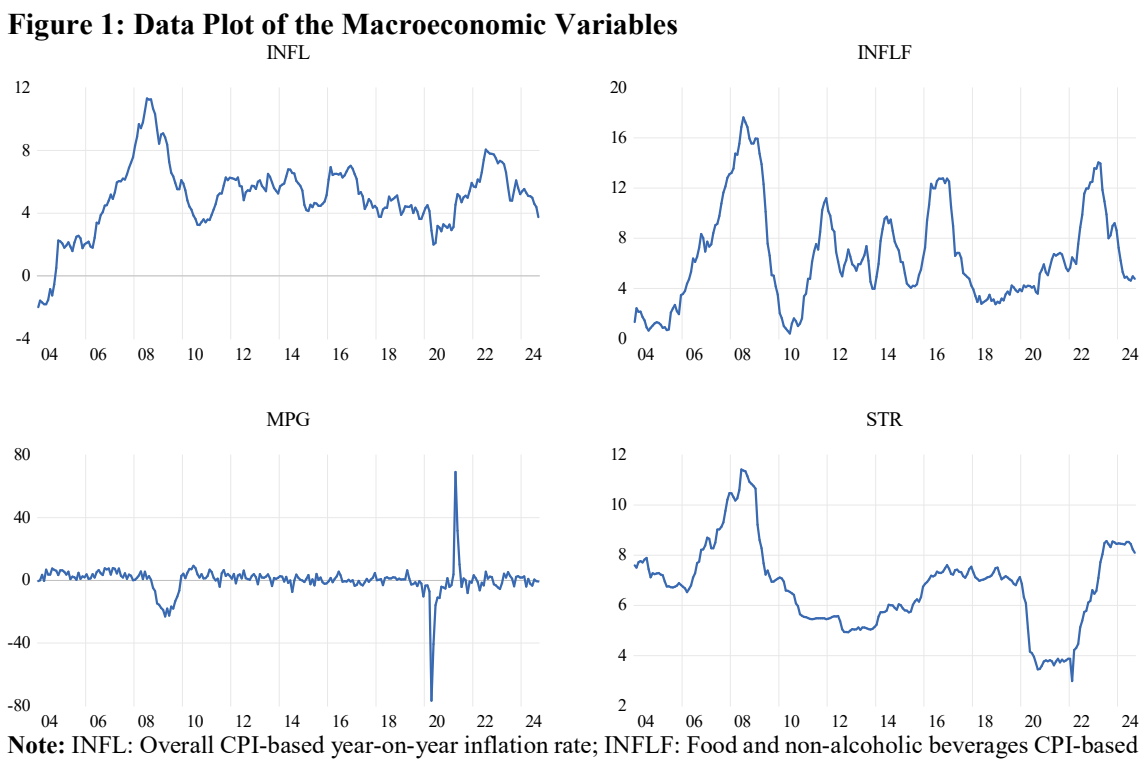
References

- AghaKouchak, A., Chiang, F., Huning, L.S., Love, C.A., Mallakpour, I., Mazdiyasni, O., Moftakhari, H., Papalexiou, S.M., Ragno, E., and Sadegh, M. (2020). Climate extremes and compound hazards in a warming world. Annual Review of Earth and Planetary Sciences, 48, 519-548.
- Alessandri, P., and Mumtaz, H. (2022). The macroeconomic cost of climate volatility. Birkbeck Centre for Applied Macroeconomics Working Paper No. 2202.
- Arteaga-Garavito, M.J., Colacito, R., Croce, M.M., and Yang, B. (2023). International Climate News. Available at: https://ssrn.com/abstract=4713016.
- Bai, J., and Perron, P. (2003). Computation and analysis of multiple structural change models. Journal of Applied Econometrics, 18(1), 1-22.
- Balcilar, M., Gupta R., Nguyen D.K., and Wohar, M.E. (2018b). Causal effects of the United States and Japan on Pacific-Rim stock markets: nonparametric quantile causality approach. Applied Economics, 50(53), 5712-5727.
- Batten, S. (2018). Climate change and the macro-economy: a critical review. Bank of England Working Paper No. 706.
- Belloni, A., Chernozhukov, V., Chetverikov, D., and Fernandez-Val, I. (2019). Conditional quantile processes based on series or many regressors. Journal of Econometrics, 213(1), 4-29.
- Ben Ameur, H., Dao, D., Ftiti, Z., & Louhichi, W. (2024). Perceived climate risk and stock prices: An empirical analysis of pricing effects. Risk Analysis. DOI: https://doi.org/10.1111/risa.17683.
- Ben Nasr, A., Balcilar, M., Ajmi, A.N., Aye, G.C., Gupta, R., and van Eyden, R. (2015). Causality between inflation and inflation uncertainty in South Africa: Evidence from a Markov-switching vector autoregressive model. Emerging Markets Review, 24(C), 46-68.
- Bilal, A., and Känzig, D.R. (Forthcoming). The Macroeconomic Impact of Climate Change: Global vs. Local Temperature. Quarterly Journal of Economics
- Bonaccolto, G., Caporin, M., and Gupta, R. (2018). The dynamic impact of uncertainty in causing and forecasting the distribution of oil returns and risk. Physica A: Statistical Mechanics and its Applications, 507(C), 446-469.
- Brock, W., Dechert, D., Scheinkman, J., and LeBaron, B. (1996). A test for independence based on the correlation dimension. Econometric Reviews, 15(3), 197-235.
- Bua, G., Kapp, D., Ramella, F., and Rognone, L. (2022). Transition versus physical climate risk pricing in European financial markets: A text-based approach. European Journal of Finance, 30(17), 2076-2110.
- Burriel, P., Kataryniuk, I., Moreno Pérez, C., and Viani, F. (2024). A New Supply Bottlenecks Index Based On Newspaper Data. International Journal of Central Banking, 20(2), 17-69.
- Cashin, P., Mohaddes, K., and Raissi, M. (2017). Fair weather or foul? The macroeconomic effects of El Niño. Journal of International Economics, 106(C), 37-54.
- Cevik, S., and Jalles, J. T. (2023). Eye of the Storm: The Impact of Climate Shocks on Inflation and Growth. International Monetary Fund Working Paper No. WP/23/87.
- Chavleishvili, S., and Moench, E. (2025). Natural disasters as macroeconomic tail risks? Journal of Econometrics, 247(C), 105914.
- Chen, Y., Wu, F., and Zhang, D. (2024). Global Climate Finance Architecture: Institutional Development. In: Climate Finance: Supporting a Sustainable Energy Transition (Series: Climate Change and Energy Transition), Edited by: Fei Wu, Dayong Zhang, and Qiang Ji, Hpater 2, 51-100. Springer Nature, Singapore.
- Ciccarelli, M., Kuik, F., and Martínez Hernández, C. (2023). The asymmetric effects of weather shocks on euro area inflation. European Central Bank Working Paper No. 2798.

- Ciccarelli, M., and Marotta, F. (2024). Demand or supply? An empirical exploration of the effects of climate change on the macroeconomy. Energy Economics, 129(C), 107163.
- Cleveland, R.B., Cleveland, W.S., McRae, J.E., and Terpenning, I. (1990). STL: A Seasonal-Trend Decomposition Procedure Based on Loess. Journal of Official Statistics, 6(1), 3-73.
- Dickey, D.A., and Fuller, W.A. (1979). Distribution of the estimators for autoregressive time series with a unit root. Journal of the American Statistical Society, 74(366), 427-431.
- Engle, R.F., Giglio, S., Kelly, B., Lee, H., and Stroebel, J. (2020). Hedging climate change news. Review of Financial Studies, 33(3), 11841216.
- Faccia, D., Parker, M., and Stracca, L. (2021). Feeling the heat: extreme temperatures and price stability. European Central Bank Working Paper No. 2626.
- Faccini, R., Matin, R., and Skiadopoulos, G. (2023). Dissecting climate risks: Are they reflected in stock prices? Journal of Banking and Finance, 155(C), 106948.
- Ferrari, A., Nispi Landi, V. (2024). Will the Green Transition be Inflationary? Expectations Matter. IMF Economic Review. DOI: https://doi.org/10.1057/s41308-024-00262-x.
- Grab, S. W. and Nash, D. J. (2024). A new flood chronology for kwazulu-natal (1836–2022): The april 2022 durban floods in historical context. South African Geographical Journal, 106(4):476–497
- Huang, B., and Teresa Punzi, M. (2024). Macroeconomic impact of environmental policy uncertainty and monetary policy implications. Journal of Climate Finance, 7(C), 100040.
- Huber, F., Krisztin, T., and Pfarrhofer, M. (2023). A Bayesian panel VAR model to analyze the impact of climate change on high-income economies. Annals of Applied Statistics, 17(2), 1543-1573.
- Hsiao, C., and Li, Q. (2001). A diagnostic test for structural stability of time-series models. Journal of Econometrics, 97(1), 107-135.
- Hsiao, C., Li, Q., and Racine, J.S. (2007). A consistent model specification test with mixed discrete and continuous data. Journal of Econometrics, 140(2), 802-826.
- Ji, Q., Ma, D., Zhai, P., Fan, Y., and Zhang, D. (2024). Global climate policy uncertainty and financial markets. Journal of International Financial Markets, Institutions and Money, 95(C), 102047.
- Kabundi, A., Mlachila, M., and Yao, J. (2022). How Persistent Are Climate-Related Price Shocks? Implications for Monetary Policy. International Monetary Fund Working Paper No. WP/22/207.
- Kim, H.S., Matthes, C., and Phan, T. (2025). Severe Weather and the macroeconomy. American Economic Journal: Macroeconomics, 17 (2), 315-341.
- Kutu, K., Das, S., and Gupta, R. (Forthcoming). Paradox of Sustainable Agricultural Policy Under Climate Change in South Africa: The Whys? and What-Ifs! In Environmental, Social and Corporate Governance and Climate Risk Management: Pathways for Sustainable Growth, Edited by Profess Kiran Yadav, Chapter 6, CRC Press, Taylor & Francis Group, LLC, Delaware, United States.
- Li, Q., and Wang, S. (1998). A simple consistent bootstrap test for a parametric regression function. Econometric Theory, 14(3), 381-399.
- Liao, W., Sheng, X., Gupta, R., and Karmakar, S. (2024). Extreme Weather Shocks and State-Level Inflation of the United States. Economics Letters, 238(C), 111714.
- Lin, B., and Zhao, H. (2023). Tracking policy uncertainty under climate change. Resources Policy, 83(C), 103699.
- López-Salido, D., and Loria, F. (2024). Inflation at risk. Journal of Monetary Economics, 145 (Supplement), 103570.
- Ma, D., Zhang, D., Guo, K., Ji, Q. (2024) Coupling between global climate policy uncertainty and economic policy uncertainty. Finance Research Letters, 69 (Part B), 106180.

- Mukherjee, K., and Ouattara, B. (2021). Climate and monetary policy: do temperature shocks lead to inflationary pressures? Climatic Change, 167(3-4), 32.
- Parker, M. (2018). The impact of disasters on inflation. Economics of Disasters and Climate Change, 2(1), 21-48.
- Plakandaras, V., Gupta, R., Balcilar, M., and Ji, Q. (2022). Evolving United States stock market volatility: The role of conventional and unconventional monetary policies. The North American Journal of Economics and Finance, 60, 101666.
- Qi, C., Ma, Y., Du, M., Ma, X., Xu, Y., and Zhou, X. (2025). Impacts of climate change on inflation: An analysis based on long and short term effects and pass-through mechanisms. International Review of Economics and Finance, 98(C), 103846.
- SARB (2025). Climate Change Policy and Regulatory Framework in the National Payment. National Payment System Department, Consultation paper, March 2025. Available at: https://www.resbank.co.za/content/dam/sarb/what-we-do/payments-and-settlements/regulation-oversight-and-supervision/document-for-comments/doc-for-comments-2025/cdi.
 - 2025/Climate%20change%20policy%20and%20regulatory%20framework%20consultation%20paper March%202025.pdf.
- Schnabel, I. (2022). A new age of energy inflation: climateflation, fossilflation and greenflation. In "Speech given at a panel on "Monetary Policy and Climate Change" at The ECB and its Watchers XXII Conference, March" 2022. Available at: https://www.ecb.europa.eu/press/key/date/2022/html/ecb.sp220317_2~dbb3582f0a.en.htm 1.
- Sheng, X., Gupta, R., and Cepni, O. (2022). Persistence of state-level uncertainty of the United States: The role of climate risks. Economics Letters, 215(C), 110500.
- Sheng, X., Gupta, R., and Cepni, O. (2024). Time-Varying effects of extreme weather shocks on output growth of the United States. Finance Research Letters, 70(C), 106318.
- Steenkamp, R., Gupta, R., and Cepni, O. (Forthcoming). Analysing the Predictability of Climate Risks on the Conditional Distributions of Bank Returns and Volatility: An International Perspective. In: Recent Developments in Computational Finance and Business Analytics, Edited by: Francesco Bartolucci, Rangan Gupta, Vasilios N. Katsikis and Srikanta Patnaik. Springer Nature, Switzerland.
- Sundaresan, S. (2024). Emergency Preparation and Uncertainty Persistence. Management Science, 70(5), 2842-2861.
- Wu, K., Karmakar, S., Gupta, R., and Pierdzioch, C. (2024). Climate Risks and Stock Market Volatility Over a Century in an Emerging Market Economy: The Case of South Africa. Climate, 12(5), 68.
- van der Westhuizen, C., van Eyden, R., and Aye, G.C. (2023). Is inflation uncertainty a self-fulfilling prophecy in South Africa? South African Journal of Economics, 91(3), 306-329.
- Zhang, Y., Liu, L., Lan, M., Su, Z., Wang, K (2024). Climate change and economic policy uncertainty: Evidence from major countries around the world. Economic Analysis and Policy, 81(C), 1045-1060.

FIGURES and TABLES:



year-on-year inflation rate; MPG: Year-on-year growth rate of manufacturing production index, and; STR: 3month Treasury bill rate.

Table 1: Climate Change Vocabulary (CCV) List for CAI-SA

Category	Keywords
Physical Risks	1. Climate
·	2. Climate change
	3. Climate risk
	4. CO ₂
	5. CO ₂ emission
	6. Carbon dioxide
	7. Carbon emission
	8. Carbon emissions
	9. Climate Adaptation
	10. Climate Resilience
	11. Climate vulnerability
	12. Ecosystem
	13. Emissions
	14. Environment
	15. Global warming
	16. Greenhouse gas
	17. Warming
Transition Risks	
Transition Risks	18. Adaptive Capacity
	19. Biological energy
	20. Biomass energy
	21. Carbon Budget
	22. Carbon capture
	23. Carbon market
	24. Carbon sequestration
	25. Carbon Sink
	26. Carbon tax
	27. Carbon Tax Act
	28. Clean energy
	29. Climate mitigation
	30. COP
	31. Disaster Management Act
	32. Emissions profile
	33. Emissions trajectory
	34. Environmental Management Act
	35. Green energy
	36. Greenhouse gas emissions inventory
	37. Hydropower
	38. IPCC
	39. Just energy transition
	40. Just transition
	41. Kyoto Protocol
	42. National Climate Change Response White Paper
	43. Nationally Determined Contribution
	44. Nuclear power
	45. Paris Agreement
	46. Presidential Climate Commission
	47. Provincial Forum on Climate Change
	48. Renewable energy
	49. Sectoral emissions targets
	50. Solar power
	51. Sustainable development
	52. UNFCCC
	53. Wind energy
	55. White energy

Note: The CCVs in italics correspond to the local SVI terms.

Figure 2: Word Cloud of Climate Change Vocabulary (CCV)

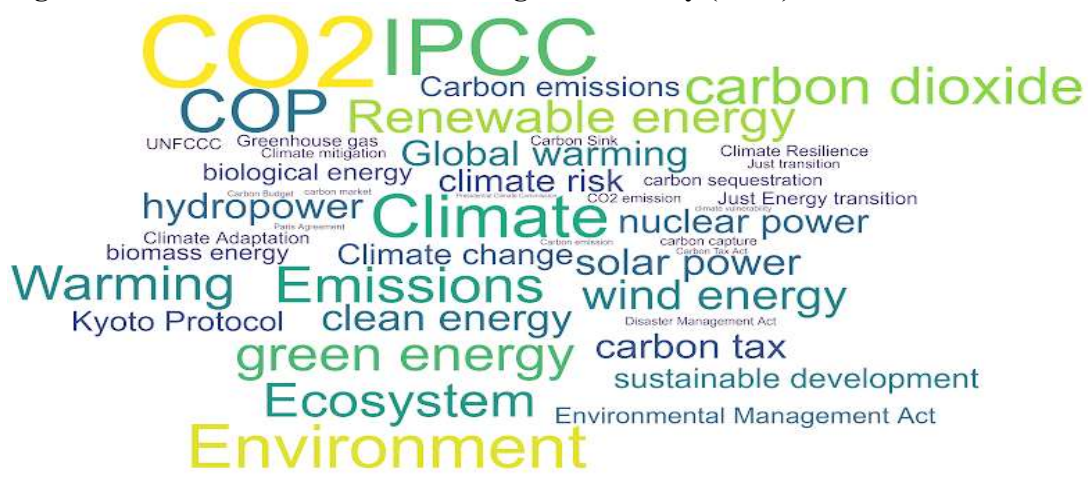


Figure 3: Climate Attention Index-South Africa (CAI-SA)

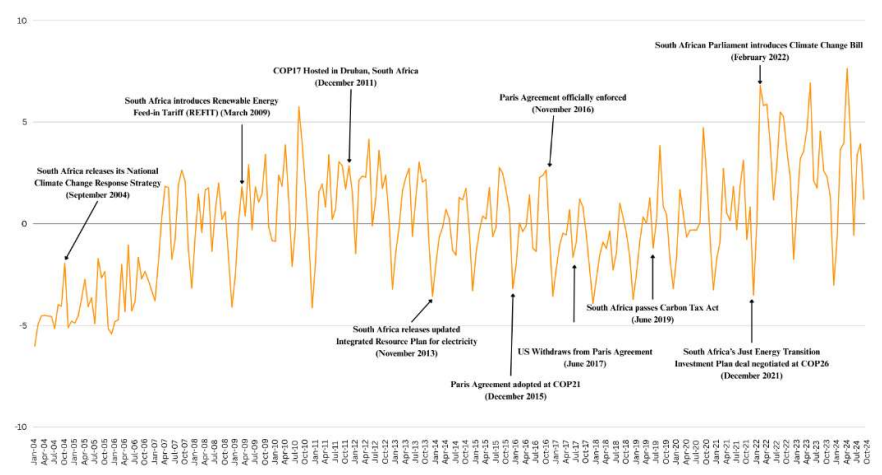


Table 2: Geographic Specification of Climate-Related Events

Geographic specificity of	Event	Date of Event
event		
Global	Paris Agreement adopted at COP 21	December 2015
	Paris Agreement officially enforced	November 2016
	US withdraws from Paris Agreement	June 2017
	US Rejoins Paris Agreement	January 2021
Local	SA releases National Climate Change	September 2004
	Response Strategy ¹⁵	
	SA introduces National Renewable	March 2009
	Energy Feed-In Tariff (REFIT) ¹⁶	
	SA releases updates Integrated Resource	November 2013
	Plan for electricity ¹⁷	
	SA passes Carbon Tax Act ¹⁸	June, 2019
	SA introduces Climate Change Bill ¹⁹	February, 2022
Transnational	SA hosts COP17 Conference in Durban	December 2011
	SA Just Energy Transition	November 2021
	Investment Plan concluded at COP26	

Table 3: Summary Statistics

Table 5. Summ	able 5. Summary Statistics					
Statistic	INFL	INFLF	MPG	STR	CAI-SA	
Mean	5.0319	6.6585	0.1747	6.7521	-0.0143	
Median	5.1251	5.9500	1.1811	6.9400	0.0108	
Maximum	11.3118	17.6400	69.1066	11.4200	6.0833	
Minimum	-1.9993	0.4000	-76.7255	2.9800	-5.8180	
Std. Dev.	2.2524	4.0128	9.0426	1.6914	2.1664	
Skewness	-0.3431	0.6951	-1.2526	0.3449	-0.2961	
Kurtosis	4.6848	2.8042	38.0237	3.3248	3.5334	
Jarque-Bera	34.3359***	20.4480***	12791.7000***	6.0300**	6.5895**	
ADF	-3.1534**	-3.2513**	-4.3533***	-3.3154**	-3.0055**	
Observations	249 (January 2004-September 2024)					

Note: INFL: Overall CPI-based year-on-year inflation rate; INFLF: Food and non-alcoholic beverages CPI-based year-on-year inflation rate; MPG: Year-on-year growth rate of manufacturing production index; STR: 3-month Treasury bill rate, and; CAI-SA: Google Trends-based Climate Attention Index of South Africa. Std. Dev. stands for standard deviation; the null hypotheses of the Jarque-Bera and the Augmented Dickey-Fuller (ADF) tests correspond to normality and unit root, respectively; *** and ** indicate rejection of the null hypothesis at the 1% and 5% levels of significance, respectively.

¹⁵ See: https://cer.org.za/wp-content/uploads/2014/05/sem sup3 south africa.pdf

¹⁶ See: https://www.gov.za/documents/notices/national-energy-regulator-south-africa-south-africa-renewable-energy-feed-tariff

¹⁷ See: https://www.gov.za/news/media-statements/media-statement-draft-irp-report-10-dec-2013

¹⁸ See: https://www.gov.za/documents/acts/carbon-tax-act-15-2019-english-afrikaans-23-may-2019

¹⁹ See: https://www.gov.za/sites/default/files/gcis document/202203/b9-2022.pdf

Table 4: Brock et al. (1996) BDS Test of Non-Linearity

Dependent Variable	m=2	m=3	m=4	m=5	m=6
INFL	3.1566***	2.8612***	2.7668***	2.4764***	2.0402**
INFLF	5.8035***	6.0633***	5.9159***	6.0598***	6.2894***

Note: See Notes to Table 1. Entries correspond to the z-statistic of the BDS test with the null of i.i.d. residuals across various dimensions (m), with the test applied to the residuals recovered from the equation of INFL or INFLF with p = 1 lag each of INFL or INFLF and CAI-SA; *** and ** indicate rejection of the null hypothesis at the 1% and 5% levels of significance, respectively.

Table 5: Multivariate kth-Order Nonparametric Causality-in-Quantiles Test Results

	Dependent Variable				
Quantile	INFL	INFLF	INFL ²	INFLF ²	
0.10	34.7424***	41.6213***	34.7627***	36.7164***	
0.20	14.5719***	18.2200***	14.3277***	15.6247***	
0.30	6.5798***	8.7033***	6.2604***	7.1454***	
0.40	2.9987***	4.0590***	2.6412***	3.1882***	
0.50	2.0926**	2.2330**	1.7003*	1.9266*	
0.60	3.5024***	2.7046***	3.0600***	2.9478***	
0.70	7.6881***	5.7702***	7.1565***	6.6498***	
0.80	16.5889***	13.0384***	15.8699***	14.8397***	
0.90	38.7639***	31.7822***	37.5057***	35.5840***	

Note: See Notes to Table 1. ***, ** and * indicate rejection of the null hypothesis of no Granger causality at the 1%, 5% and 10% level of significance respectively (given the corresponding critical values of 2.575, 1.96 and 1.645 for the standard normal test statistic) from CAI-SA to INFL, INFLF, INFLF for a particular quantile, with INFL or INFLF capturing volatility.

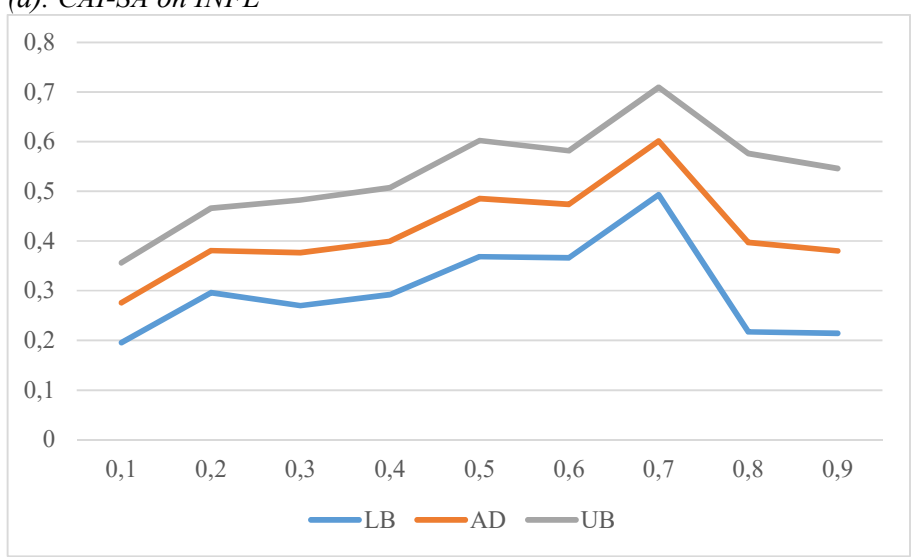
Table 6: Multivariate Bootstrapped kth-Order Nonparametric Causality-in-Quantiles Test Results

	Dependent Variable				
Quantile	INFL	INFLF	INFL ²	INFLF ²	
0.10	19.8296	14.8764	15.7985	19.4243	
0.20	5.8213	10.6425	6.9261	6.3515	
0.30	4.0858	4.1673	3.6036	3.6927	
0.40	2.6850	3.1277	2.9149	2.4769	
0.50	1.9489	2.9296	2.1961	2.3574	
0.60	2.2180	3.6806	3.0111	1.9699	
0.70	3.0858	4.9220	4.8311	3.0279	
0.80	8.3895	6.1597	7.8360	7.9025	
0.90	17.7284	13.1330	17.6184	18.7596	

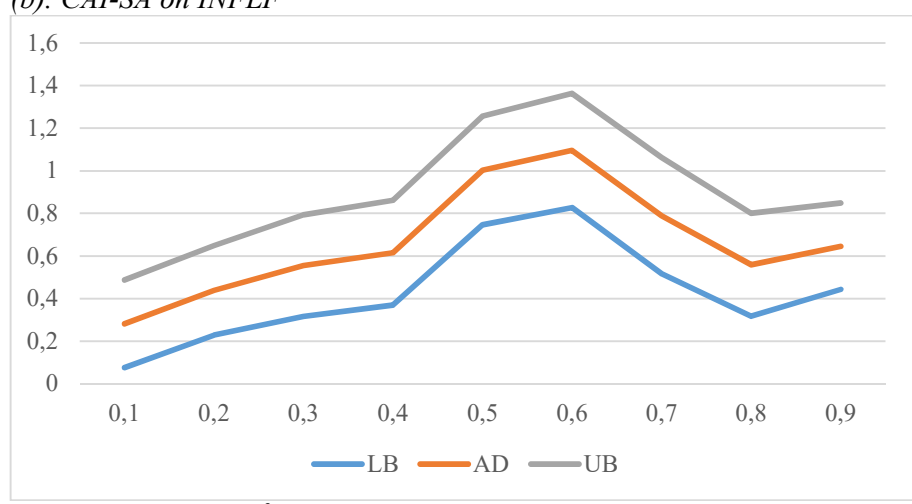
Note: See Notes to Table 1. The entries correspond to the quantile-specific 5% bootstrapped critical values for the null hypothesis of no Granger causality from CAI-SA to INFL, INFLF, INFL², or INFLF² for a particular quantile, with INFL² or INFLF² capturing volatility.

Figure 4: Average Derivative Estimates

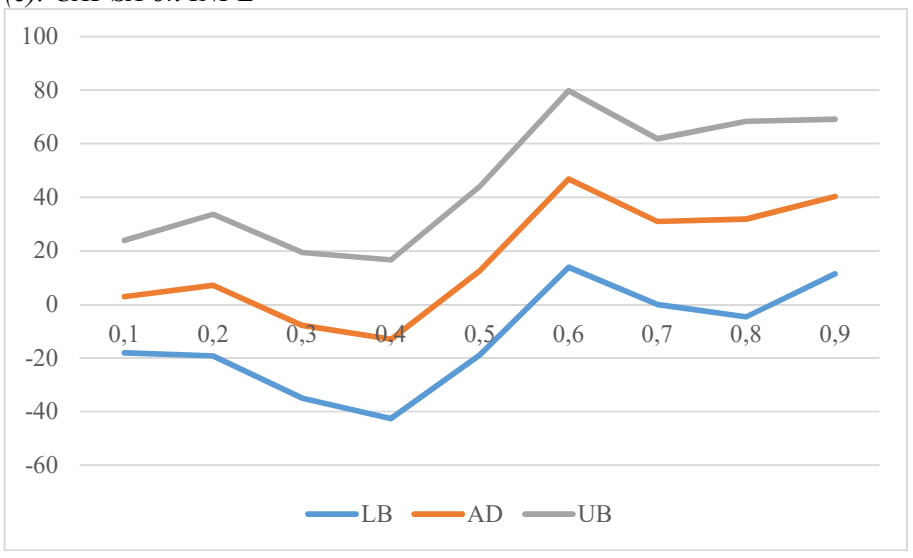
(a). CAI-SA on INFL

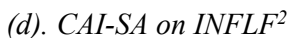


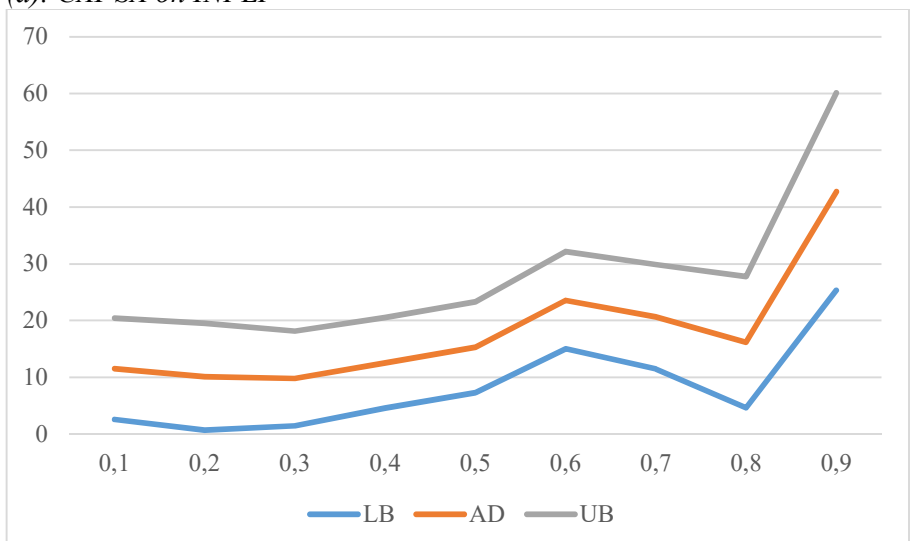
(b). CAI-SA on INFLF



(c). CAI-SA on INFL²







Note: See Notes to Figures 1 and 2. The figures plot the average derivative (AD) estimates of the sign of the effect of CAI-SA on INFL, INFLF, INFL², or INFLF² in the *k*-th-order multivariate nonparametric causality-in-quantiles models for a particular quantile (horizontal axis), with INFL² or INFLF² capturing volatility, and LB and UB corresponding to 95% lower and upper bound, respectively.

APPENDIXES:

Appendix A. Additional Results

Table A1: Bivariate k-th-Order Nonparametric Causality-in-Quantiles Test Results

	Dependent Variable			
Quantile	INFL	INFL ²		
0.10	32.3095***	34.7921***		
0.20	13.9959***	15.0879***		
0.30	6.7598***	7.1989***		
0.40	3.5077***	3.4875***		
0.50	2.6459***	2.2230**		
0.60	3.8347***	2.9952***		
0.70	7.4724***	6.1273***		
0.80	15.2745***	13.1795***		
0.90	34.8405***	31.1432***		

Note: See Notes to Table 1. *** and ** indicate rejection of the null hypothesis of no Granger causality at the 1% and 5% level of significance respectively (given the corresponding critical values of 2.575 and 1.96 for the standard normal test statistic) from CAI-SA to INFL or INFL² for a particular quantile, with INFL² capturing volatility.

Table A2: Multivariate k-th-Order Nonparametric Causality-in-Quantiles Test Results

	Dependent Variable			
Quantile	MPG	MPG^2		
0.10	22.6136***	21.1749***		
0.20	10.4493***	9.8701***		
0.30	5.7339***	5.5687***		
0.40	3.7843***	3.9089***		
0.50	3.5690***	3.9483***		
0.60	4.9155***	5.5629***		
0.70	8.2059***	9.1876***		
0.80	14.9004***	16.3882***		
0.90	31.4347***	33.9723***		

Note: See Notes to Table 1. *** indicate rejection of the null hypothesis of no Granger causality at the 1% level of significance (given the corresponding critical value of 2.575 for the standard normal test statistic) from CAI-SA to MPG or MPG² for a particular quantile, with MPG² capturing volatility.

Table A3: Multivariate kth-Order Nonparametric Causality-in-Quantiles Test Results

	Dependent Variable				
	INFL	$INFL^2$	INFL	INFL ²	
Quantile	Predictor: C	CAI-SA-Avg.	Predictor: CAI-SA-WtdAv		
0.10	21.9636***	18.0320***	36.4578***	37.9382***	
0.20	10.8677***	8.6405***	14.9482***	15.7107***	
0.30	6.7081***	5.1811***	6.5430***	6.9302***	
0.40	4.9626***	3.8490***	2.8346***	2.9448***	
0.50	4.6574***	3.8419***	1.9524*	1.8169*	
0.60	5.6085***	5.0464***	3.5072***	3.1211***	
0.70	8.1073***	7.8053***	7.9815***	7.3018***	
0.80	13.3360***	13.3844***	17.4168***	16.3257***	
0.90	26.5857***	27.4106***	40.7949***	38.8999***	

Note: See Notes to Table 1. *** and * indicate rejection of the null hypothesis of no Granger causality at the 1% and 10% level of significance respectively (given the corresponding critical values of 2.575 and 1.645 for the standard normal test statistic) from the simple average-based CAI (CAI-SA-Avg.) or the weighted average-based CAI (CAI-SA-Wtd.-Avg.) to INFL or INFL² for a particular quantile, with INFL² capturing volatility.

Table A4: Bivariate kth-Order Nonparametric Causality-in-Quantiles Test Results

	Dependent Variable				
	INFL	INFL ²	INFL	INFL ²	
Quantile	Predictor:	CAI-SA-Alt.	Predictor	: CAI-SA	
0.10	0.3026	1.1430	0.3026	1.3615	
0.20	0.4775	1.4602	0.5943	1.6105	
0.30	0.9757	0.8763	2.1080**	2.1080**	
0.40	0.7733	0.7180	2.4460**	2.4460**	
0.50	0.4733	0.4733	2.8605***	2.6559***	
0.60	0.5340	0.3700	2.2964**	2.2964**	
0.70	0.3626	0.3265	2.0044**	2.0044**	
0.80	0.6600	1.9407*	0.6172	1.9598*	
0.90	0.3984	1.5649	0.2964	1.5649	

Note: See Notes to Table 1. ***, ** and * indicate rejection of the null hypothesis of no Granger causality at the 1%, 5% and 10% level of significance respectively (given the corresponding critical values of 2.575, 1.96 and 1.645 for the standard normal test statistic) from the Twitter-based CAI (CAI-SA-Alt.) or the CAI-SA to INFL or INFL² for a particular quantile, with INFL² capturing volatility.

Appendix B. Technical Details of a Residual-Based Bootstrap Procedure for the Quantile Causality Test

We consider a single quantile level θ for simplicity, though the procedure may be applied separately for any $\theta \in (0,1)$ of interest (e.g. to test for causality at multiple quantiles).

Next, we describe the residual-based bootstrap algorithm for the causality-in-quantiles test statistic, following the approach outlined by Hsiao and Li (2001). The objective is to simulate the distribution of \hat{f}_T under the null hypothesis (u_t does not affect v_t 's θ -quantile) and to use the simulated distribution to calibrate the test. The steps involved are as follows:

1. Estimate the θ -quantile model under H_0 : Based on the observed data $\{u_t, Z_{t-1}\}_{t=1}^T$, estimate the conditional quantile function $Q_{\theta}(u_t \mid Z_{t-1} \setminus V_{t-1})$ (excluding v_t). This may be accomplished by local linear quantile regression. More precisely, let $X_{t-1} \equiv Z_{t-1} \setminus V_{t-1}$ be the p-lag vector excluding the v variables. For every point x in the support of X_{t-1} , the local linear estimator $(\hat{q}_0(\theta, x), \hat{q}_{x'}(\theta, x))'$ is found by solving

$$\min_{q_0,q_x} \sum_{t=v+1}^{T} \rho_{\theta} (u_t - q_0 - q_{\chi'}(X_{t-1} - v)) L\left(\frac{X_{t-1} - v}{b}\right),$$

where $\rho_{\theta}(e) = [\theta, 1\{e \geq 0\} - (1-\theta)1\{e < 0\}]e$ is the check loss function of quantile regression. This optimization delivers $\hat{q}_0(\theta, x)$ (the fitted θ -quantile at $X_{t-1} = x$) and $\hat{q}_x(\theta, x)$ (a vector of slopes) for each local neighborhood about x. Specifically, for each observation t, the fitted conditional quantile for u_t is $\hat{Q}_{\theta}(Z_{t-1} \setminus V_{t-1}) = \hat{q}_0(\theta, X_{t-1})$. Based on this fitted function, calculate the *residuals* for t = p + 1, ..., T as

$$\hat{\epsilon}_t(\theta) = u_t - [\hat{q}_{0,t}(\theta) + \hat{q}_{x,t'}(\theta)X_{t-1}],$$

where we use the notation $\hat{q}_{0,t}(\theta) \equiv \hat{q}_0(\theta, X_{t-1})$ and $\hat{q}_{x,t}(\theta) \equiv \hat{q}_x(\theta, X_{t-1})$ for convenience.

- 2. Resample centered residuals: As the $\hat{\epsilon}_t(\theta)$ from above may not have zero mean (they are quantile residuals, and not ordinary least squares residuals), we first recentre them to impose the null condition of zero average effect. Let $\bar{\epsilon} = \frac{1}{T-p} \sum_{t=p+1}^T \hat{\epsilon}_t(\theta)$ denote the sample mean of the residuals. Define the centered residuals $\tilde{\epsilon}_t = \hat{\epsilon}_t(\theta) \bar{\epsilon}$. We then take a bootstrap sample $\{\hat{\epsilon}_t^*(\theta)\}_{t=p+1}^T$ of T-p values by sampling with replacement from the centered residuals $\{\tilde{\epsilon}_t\}$. This provides a resampled error series $\hat{\epsilon}_t^*(\theta)$ that replicates the distribution of the quantile regression errors under H_0 . (We keep the same sample size T in each bootstrap replication.)
- 3. Recursive generation of a bootstrap series $\{u_t^*\}$: Based on the resampled errors from Step 2, we generate a synthetic time series $\{u_t^*\}_{t=1}^T$ under the null hypothesis. The bootstrap series is generated recursively according to the estimated quantile model. We begin by setting the first p values $u_1^*, ..., u_p^*$ to the real observed values of u (this fixes the simulation at a realistic starting point). Then, for each t = p + 1, p + 2, ..., T, we calculate

$$u_t^* = \hat{q}_{0,t}(\theta) + \hat{q}_{x,t'}(\theta)X_{t-1}^* + \hat{\epsilon}_t^*(\theta),$$

where $X_{t-1}^* \equiv Z_{t-1}^* \setminus V_{t-1}^*$ is the bootstrap counterpart of X_{t-1} . Practically, this implies that X_{t-1}^* contains the lagged values of the new series $\{u^*\}_{t=1}^T$ (and any other control variables w_t if any), but *not* v as we are simulating under H_0 .

- 4. Calculate the bootstrap test statistic: Once we have generated a bootstrap sample in Step 3, we compute its quantile-causality test statistic \hat{J}_T^* in the same manner as the original \hat{J}_T . That is, we calculate equation (6) on the bootstrap sample $\{\hat{c}_t^*(\theta), Z_{t-1}^*\}$.
- 5. Repeat and invert the bootstrap distribution: We replicate Steps 2-4 a total of B times (with independent resampling in each replication) to create B bootstrap statistics $\{\hat{J}_{T,b}^*\}_{b=1}^B$. These values comprise an empirical approximation to the sampling distribution of \hat{J}_T under H_0 . Finally, we can extract a bootstrap p-value or critical values from this distribution. For instance, the α -percent critical value, $\hat{c}_{1-\alpha}$, is simply the $(1-\alpha)$ -quantile of the empirically generated bootstrap statistics, which is obtained as:

$$\hat{c}_{1-\alpha} = \inf\{a: \frac{1}{B} \sum_{b=1}^{B} \mathbf{1} (\hat{J}_{T,b}^* \le a) \ge 1 - \alpha\}.$$

As the bootstrap replicates the null, it provides a better reflection of the finite-sample variability of \hat{J}_T than the large-sample theory. Specifically, studies have shown that the bootstrap test achieves empirical size much closer to nominal and has greater power than the asymptotic test in finite samples. By not relying on the slow asymptotic approximations, the bootstrap approach enhances the reliability of the test across quantiles in finite samples, as first shown by Li and Wang (1998) and Hsiao and Li (2001). The aforementioned bootstrap algorithm is implemented for a given quantile level θ . In practice, one can implement the same algorithm for each quantile of interest (e.g. $\theta = 0.1,0.5,0.9$, etc.) separately, obtaining potentially different \hat{J}_T statistics and bootstrap critical values at each θ . We fix B = 399 in the empirical application, since computational cost is prohibitive for larger values of B.